

Metastable states in the $J_1 - J_2$ Ising model

V. A. Abalmasov^{1,*} and B. E. Vugmeister^{2,†}

¹*Institute of Automation and Electrometry SB RAS, 630090 Novosibirsk, Russia*

²*Datamir, Inc., Clifton, NJ 07012, USA*

Competing interactions of nearest and next-nearest-neighbor electron spins on a lattice with coupling constants J_1 and J_2 , respectively, give the system some interesting and unusual properties and may even underlie high temperature superconductivity according to the resonant valence bond theory. Here we study the $J_1 - J_2$ Ising model on the square lattice using the Random local field approximation (RLFA) and Monte Carlo (MC) simulations for various values of the ratio $p = J_2/|J_1|$. We show that the accuracy of the RLFA is comparable to the mean field cluster approximation, but, in addition, and most surprisingly, the RLFA predicts metastable states with zero polarization at low temperature for $p \in (0, 1)$. This is confirmed by our MC simulations, in which the system reaches these states after the energy relaxation of initially randomly oriented spins. Furthermore, in a moderate external field, the MC simulations reveal the existence of still other metastable states with nonzero polarizations. These findings could be crucial for explaining the magnetic and electric properties of materials, in particular, under ultrafast nonequilibrium conditions.

In recent years, many compounds have been discovered in which electron spins-1/2 form a two-dimensional square lattice and interact with their nearest and diagonal next-nearest neighbors via isotropic exchange interaction with the constants J_1 and J_2 , respectively (Fig. 1) [1, 2]. This includes also the parent compound of the high-temperature superconductivity La_2CuO_4 [3] and is likely relevant to the mechanism of the high-temperature superconductivity of the iron pnictides [4]. The corresponding Heisenberg model has been studied extensively by a variety of methods, e.g. [5]. For the values of the ratio $p = J_2/|J_1|$ near $p_0 = 1/2$, where two different ordered states have the same energy, the quantum spin liquid ground state was predicted [1, 6, 7], which may be the key to solving the problem of high-temperature superconductivity according to the resonating valence bond theory [8]. This ground state has recently been observed experimentally in several compounds [2, 9], and another exotic nematic ground state at high magnetic field has also been reported [10].

The $J_1 - J_2$ Ising model, in which spins can only point in two directions, up and down, has also been thoroughly studied theoretically using cluster mean field theory [11–13], Monte Carlo (MC) simulations [11, 14–16], and accurate tensor network simulations [17]. The nematic phase was also predicted for moderate external fields [18, 19]. Although its implementations seem less common in nature, the easier to study the $J_1 - J_2$ Ising model nonetheless is interesting in its own right, and can also shed light on some properties of its more complex Heisenberg counterpart. This is especially true for the Ising model in a transverse field, where quantum fluctuations induce gap between two phases around p_0 [13, 19–21] with the valence-bond-solid state predicted [20]. Indeed, the phase diagrams of both models have a lot in common [1, 2, 7, 13].

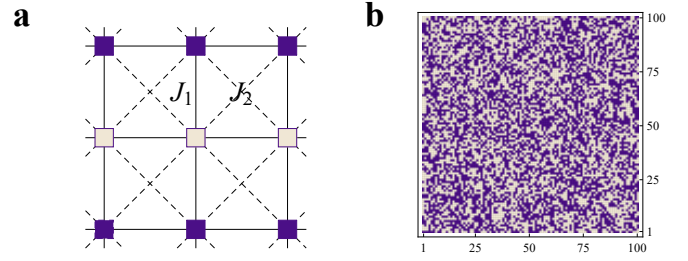


Fig. 1 | The $J_1 - J_2$ Ising model scheme. **a**, Square lattice of Ising spins (white - up, blue - down) with the interaction constant J_1 between nearest neighbors along horizontal and vertical (solid) lines and J_2 between next-nearest-neighbors along (dashed) diagonals. **b**, Random (very high temperature) spin configuration; the number of spins along each side of the square sample is $L = 100$.

At present, MC simulations can be used to calculate model properties with very high accuracy, nevertheless, easy-to-implement, adequate and efficient approximations are highly desirable to quickly and reliably determine the most salient system properties. Here we use the Random local field approximation (RLFA) [22] to study the phase transition in the $J_1 - J_2$ Ising model on the square lattice. We show that the RLFA reveals metastable states with zero uniform for $p \in (0, p_0)$ and staggered for $p \in (p_0, 1)$ polarization at low temperature. We then confirm this finding with our MC simulation and discuss the properties of these states.

We thus consider the Hamiltonian

$$H = J_1 \sum_{\langle i,j \rangle} s_i s_j + J_2 \sum_{\langle\langle i,j \rangle\rangle} s_i s_j - \sum_i h_i s_i, \quad (1)$$

where the sums are over nearest $\langle i, j \rangle$ and next-nearest (diagonal) $\langle\langle i, j \rangle\rangle$ neighbors (see Fig. 1a), as well as over each spin coupled to the external field h_i at its position; $s_i = \pm 1$. In what follows, we set ferromagnetic (FM) $J_1 = -1$ and antiferromagnetic (AFM) $J_2 = p > 0$ cou-

* abalmasov@iae.nsc.ru

† vugmeister@datamir.net

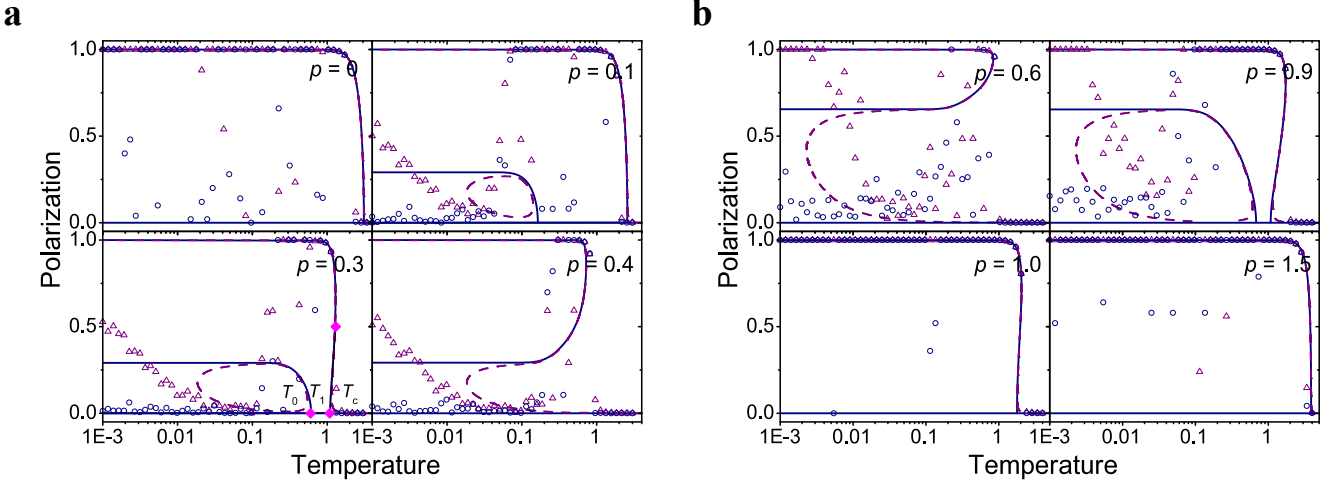


Fig. 2 | Polarization as a function of temperature obtained using the RLFA analytical approach and MC simulations. **a**, Solution of the RLFA equation (lines) and MC results (markers) for uniform polarization in a uniform field, $p < p_0$, and **b**, for staggered polarization in a staggered field, $p > p_0$. The magnitude of the field is $h = 0.001$ (purple dashed line and triangles) and $h = 0$ (blue solid line and circles). Each data point is derived from a single MC run with a random initial state at each temperature. The magenta diamonds in the bottom left panel (a) indicate the temperatures $T_0 < T_1 < T_c$.

pling constants, providing together the frustration of the system. For this choice of couplings, the ground state is FM at $p < p_0$ (being AFM with Néel checkerboard order for $J_1 > 0$) and striped or super- AFM at $p > p_0$; at $p = p_0$ the ground state is not ordered.

The starting point of the RLFA is the exact formula for the average spin value [22]:

$$\langle s_i \rangle = \langle \tanh \beta (h_i^s + h_i) \rangle, \quad (2)$$

where $\beta = 1/T$ is the inverse temperature (in energy units), $h_i^s = \sum_j J_{ij} s_j$ is the local field acting on the spin s_i due to neighboring spins s_j ; the brackets stand for the thermal averaging.

In contrast to the Mean field approximation (MFA), the spins on the right-hand side of Eq. (2) are not fixed to their mean value m . The averaging in Eq. (2) is carried out with the product of the probability distributions for each spin [23]:

$$P(s_i) = (1 + m_i s_i)/2, \quad (3)$$

where $m_i = \langle s_i \rangle = m e^{i\mathbf{q}\cdot\mathbf{r}_i}$ is the thermally averaged polarization at the position \mathbf{r}_i determined by the propagation vector \mathbf{q} . The uniform polarization corresponds to $\mathbf{q} = (0, 0)$, while the staggered polarization refers to the vectors $(0, \pi)$ and $(\pi, 0)$. The same applies to the spatial dependence of the external field h_i .

Eqs. (2) and (3) together constitute the essence of the RLFA. Eq. (2), which is a seventh degree polynomial in m according to the eight neighbor spins in the model, can be solved numerically.

The solution of the RLFA equation for uniform (at $p < p_0$) and staggered (at $p > p_0$) polarization is shown

in Fig. 2. This solution corresponds to the zero value of the Landau potential derivative with respect to m and, therefore, corresponds to its local minimum (stable or metastable state), local maximum or inflection point (unstable states). In the absence of an external field, zero polarization is always a solution to the equation, and it is unique and stable at high temperatures. At zero temperature, there is always (except in the case of $p = p_0$) another solution $m = 1$, which corresponds to full polarization and supposed to be stable. And there is still a third solution about $m \approx 0.29$ for $p \in (0, p_0)$ and $m \approx 0.65$ for $p \in (p_0, 1)$. It is natural to assume that it corresponds to a local maximum of the Landau potential separating two local minima at $m = 1$ and $m = 0$, the first of which is a stable solution, and the second is a metastable one. In an external field, the metastable state exists only in a certain temperature window (dashed purple lines in Fig. 2) and completely disappears at fields above $h \simeq 0.01$.

The phase diagram for the $J_1 - J_2$ Ising model obtained using the RLFA is shown in Fig. 3a. The critical temperatures obtained from the maxima of the dielectric susceptibility in the MC simulation (see Methods) are in good agreement with the literature data [14, 16]. In the RLFA, the transition turns out to be of the first order for p from about 0.25 up to 1.25, while recently it has been shown to be of the second order everywhere using the tensor network simulation technique [17], which apparently resolves the long-standing dispute about the order of the phase transition at $p > p_0$ [15]. The agreement of the RLFA with MC results is good for $p > p_0$. At these points, the rise of polarization is steep enough, resulting in smaller fluctuations, which are neglected by the RLFA. However, at p just below p_0 , the discrepancy turns out to be significant, with the critical temperature deter-

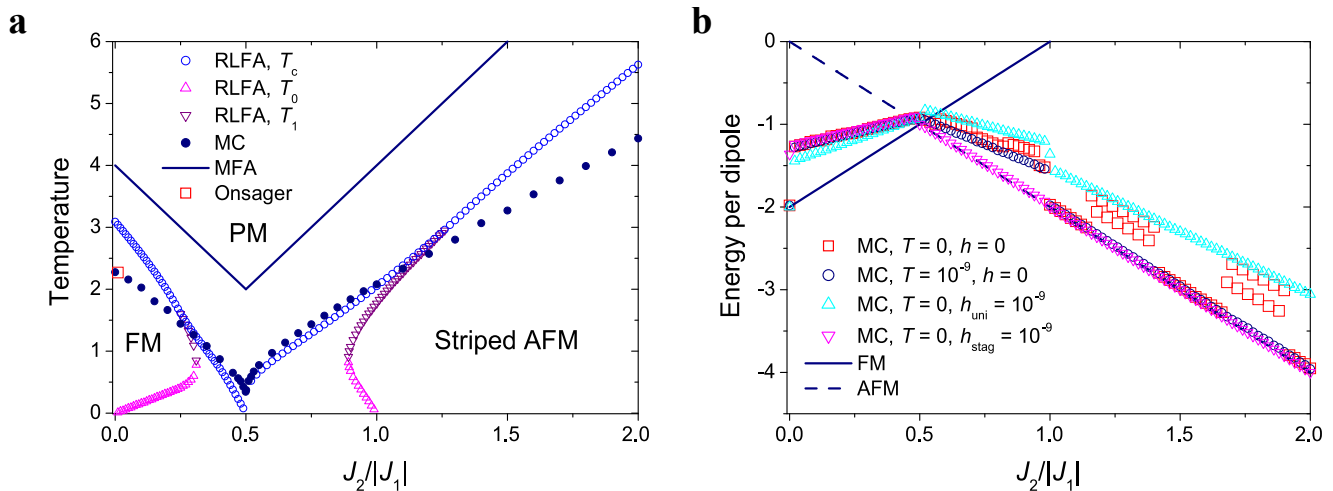


Fig. 3 | Critical temperatures and energies in the $J_1 - J_2$ Ising model as functions of $p = J_2/|J_1|$. **a**, Phase diagram obtained using the RLFA, MFA and MC. Solid dark blue curves correspond to the mean-field approximation, open blue circles, magenta up-triangles and purple down-triangles are T_c , T_0 and T_1 obtained within RLFA (Fig. 2a). The red square is the exact Onsager’s solution for the 2D Ising model. Dark blue filled circles are calculated using the MC method. **b**, Energy per dipole obtained using MC simulation at zero temperature in the absence of a field (red squares), at a temperature $T = 10^{-9}$ and a field $h = 0$ (blue circles) and $T = 0, h = 10^{-9}$ (cyan up-triangles for uniform and magenta down-triangles for staggered field). Each data point is averaged over 100 samples (see Methods). Standard deviations of the energy distribution histogram over 100 samples for each data point are smaller than the markers (Extended Data Fig. 3). Blue solid and dashed lines correspond to the energy of the FM and AFM states, respectively.

mined by the RLFA going almost linearly to zero, where it should have a finite value. In Fig. 3a, we also traced the temperatures T_0 and T_1 (see Fig. 2a, left bottom panel), which indicate the range of the zero-polarization metastable state and the temperature of the first-order phase transition in the absence of an external field. The overall accuracy of the RLFA turns out to be comparable to the commonly used cluster MFA [11–13].

It should be noted that neither staggered for $p \in (0, p_0)$ nor uniform for $p \in (p_0, 1)$ polarizations with $m = 1$ are solutions to the RLFA equation, although they are very close to it. At the same time, these states are metastable at zero temperature. Indeed, any spin flip in these states leads to an increase in energy.

To further explore the metastable states, we perform MC simulations with single-spin-flip dynamics (see Methods), making a deep quench from a high-temperature (random) spin configuration. It was previously shown that under these conditions a 2D Ising system (with $p = 0$) on a square lattice at zero temperature reaches either a frozen stripe state (Fig. 4a) with a probability of about 1/3 or a fully polarized ground state with a probability near 2/3 [24]. Later, this behavior and the probability of the occurrence of a metastable state were explained by revealing a deep connection between the zero-temperature coarsening with critical continuum percolation [25, 26].

In the absence of an external field, MC simulations do indeed show zero-polarization metastable states, even though at temperatures several times lower than follows from the RLFA (Fig. 2). Typical spin configurations of

these states at zero temperature are shown in Figs. 4b, 4f. For $p \in (0, p_0)$ the real-space correlation function of these states is exponential and the correlation length is about $l_c \approx 1.8$ with no apparent dependence on p . The result is the same when the initial state at each temperature is AFM for $p \in (0, p_0)$ or FM for $p \in (p_0, 1)$.

Surprisingly, for a small external field (uniform for $p < p_0$ and staggered for $p > p_0$) at low temperature, these states do not relax to the ground state, as it would be according to the RLFA, but get stuck instead in other metastable states (Fig. 2). At zero temperature, these metastable states appear already in an infinitesimally low external field (down to 10^{-9}) with their typical configurations shown in Figs. 4c, 4h. The polarization of these states is about $m \approx 0.5$ for $p < p_0$, and very close to $m = 1$ for $p > p_0$. It first decreases with increasing temperature, and then increases to $m = 1$ in both cases in accordance with the RLFA solution. When a uniform field is applied for $p > p_0$, which is an experimentally relevant situation, the system relaxes into even other metastable states, see Fig. 4g.

We note that some data with an intermediate polarization value in Fig. 2 actually correspond to incompletely relaxed FM and AFM states divided into slowly relaxing large domains (Figs. 4a, 4e). At the same time, the energy of these states does not differ much from a completely ordered state, but it is significantly higher for truly disordered states (Extended Data Fig. 1).

Thus, we plot the energy per dipole at zero temperature as a function of p (Fig. 3b), where the metastable states at $p \in (0, 1)$ (red squares) are clearly visible. For

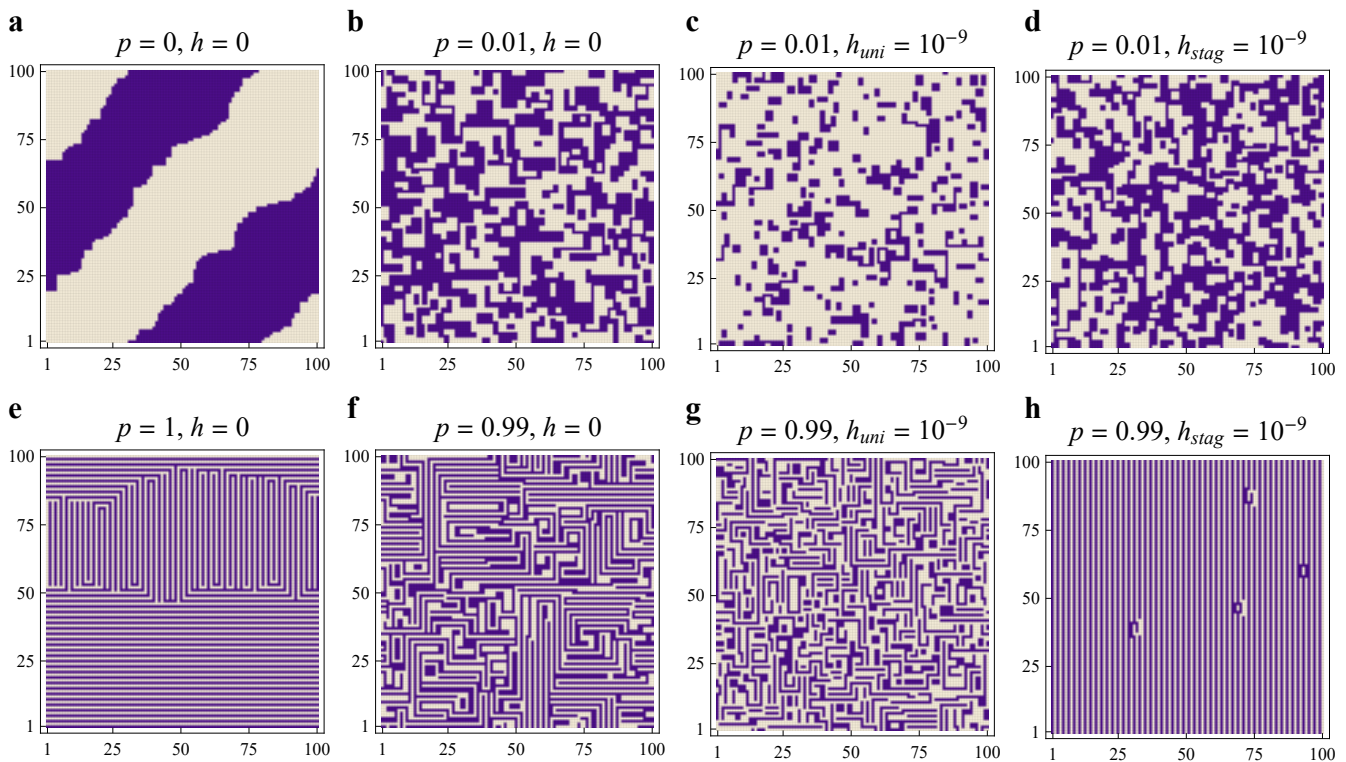


Fig. 4 | Spin configuration in relaxed states at zero temperature. Examples of spin configurations of final absorbing states after energy relaxation, starting from a random spin configuration, has been performed in the absence or in a very small uniform or staggered external field h for the values of $p = J_2/|J_1|$ equal to 0, 0.01, 0.99, and 1.

some values of $p > p_0$, the energy of metastable states in Fig. 3b appears to be slightly higher and goes above the general trend. However, it suffices to apply an infinitely small temperature of $T \sim 10^{-9}$ for these states to quickly relax into “strong” metastable states for $p \in (p_0, 1)$ or stable states for $p > 1$. Similar to the 2D Ising model ($p = 0$) [24], relaxation of strong metastable states into the ground FM or AFM states is apparently determined by the activation energy E_a as $\tau \simeq L^3 \exp(-E_a/T)$ and occurs at temperatures of the order of $T \simeq 0.1$ (Extended Data Fig. 2). Fig. 3b also shows the effect of a small external field (up- and down triangles), which we discussed above. At zero temperature, relaxation to the ground state occurs in electric fields higher than about $h \simeq 0.1$ (Extended Data Fig. 2).

The metastable states discussed here should also exist in a moderate transverse external field, and therefore they could be equally expected in the Heisenberg quantum model relating to magnetism in high-temperature superconductors [3, 4], depending on p , however. For $p \in (p_0, 1)$, metastable states with zero staggered polarization can be achieved by polarization in a uniform magnetic field and subsequent relaxation in the absence of a field at low temperature. A suitable compound is

BaCdVO(PO₄)₂ with $J_1 = -3.6$ K and $J_2 = 3.2$ K [10], which gives $p \simeq 0.9$. However, the expected temperature of metastable states is approximately two orders of magnitude lower than the already low phase transition temperature $T_N = 1.05$ K [10] (Fig. 2b and Extended Data Fig. 1). For $p \in (0, p_0)$, which is the case of VOMoO₄, PbVO₃ [1], and Sr₂Cu(Te_{1-x}W_x)O₆ [27] compounds, metastable states with zero uniform polarization can possibly be revealed in ultrafast light-pump experiments under highly nonequilibrium conditions, such as [28]. We also note that metastable states have recently been reported in incipient ferroelectric SrTiO₃ under high-intensity THz pumping [29, 30].

In conclusion, using the Random local field approximation, we predict the existence of metastable states with zero polarization in the $J_1 - J_2$ Ising model at low temperature, which is further confirmed by our Monte Carlo simulation. In a small external field, our MC simulations also reveal metastable states with non-zero polarization. These findings may be crucial for explaining the magnetic and electric properties of materials and may directly manifest themselves, in particular, under the nonequilibrium conditions of modern experiments with high-power ultrashort light pumping.

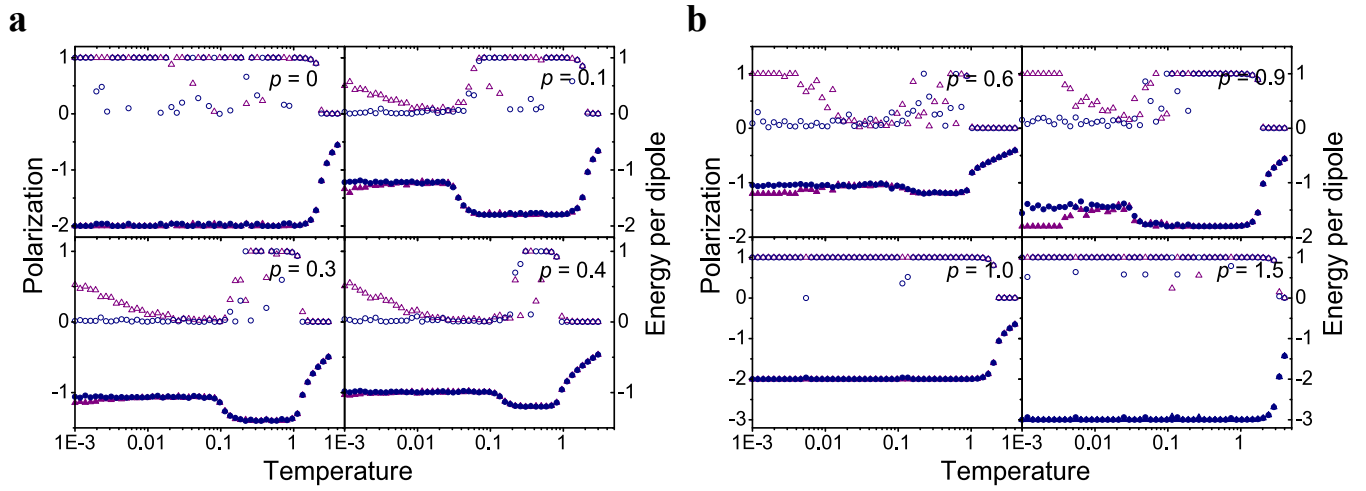
- [1] H. Ishikawa, N. Nakamura, M. Yoshida, M. Takigawa, P. Babkevich, N. Qureshi, H. M. Rønnow, T. Yajima, and Z. Hiroi, J_1 - J_2 square-lattice Heisenberg antiferromagnets with $4d^1$ spins: AMoOPO_4Cl ($A=\text{K,Rb}$), *Physical Review B* **95**, 064408 (2017).
- [2] O. Mustonen, S. Vasala, E. Sadrollahi, K. P. Schmidt, C. Baines, H. C. Walker, I. Terasaki, F. J. Litterst, E. Baggio-Saitovitch, and M. Karppinen, Spin-liquid-like state in a spin-1/2 square-lattice antiferromagnet perovskite induced by $d^{10} - d^0$ cation mixing, *Nature Communications* **9**, 1085 (2018).
- [3] R. Coldea, S. M. Hayden, G. Aeppli, T. G. Perring, C. D. Frost, T. E. Mason, S.-W. Cheong, and Z. Fisk, Spin Waves and Electronic Interactions in La_2CuO_4 , *Physical Review Letters* **86**, 5377 (2001).
- [4] Q. Si, R. Yu, and E. Abrahams, High-temperature superconductivity in iron pnictides and chalcogenides, *Nature Reviews Materials* **1**, 16017 (2016).
- [5] J.-F. Yu and Y.-J. Kao, Spin- $\frac{1}{2}$ J_1 - J_2 Heisenberg antiferromagnet on a square lattice: A plaquette renormalized tensor network study, *Physical Review B* **85**, 094407 (2012).
- [6] L. Balents, Spin liquids in frustrated magnets, *Nature* **464**, 199 (2010).
- [7] H.-C. Jiang, H. Yao, and L. Balents, Spin liquid ground state of the spin- $\frac{1}{2}$ square J_1 - J_2 Heisenberg model, *Physical Review B* **86**, 024424 (2012).
- [8] P. W. Anderson, The Resonating Valence Bond State in La_2CuO_4 and Superconductivity, *Science* **235**, 1196 (1987).
- [9] J. Wen, S.-L. Yu, S. Li, W. Yu, and J.-X. Li, Experimental identification of quantum spin liquids, *npj Quantum Materials* **4**, 12 (2019).
- [10] K. Y. Povarov, V. K. Bhartiya, Z. Yan, and A. Zheludev, Thermodynamics of a frustrated quantum magnet on a square lattice, *Physical Review B* **99**, 024413 (2019).
- [11] S. Jin, A. Sen, W. Guo, and A. W. Sandvik, Phase transitions in the frustrated Ising model on the square lattice, *Physical Review B* **87**, 144406 (2013).
- [12] A. Bobák, T. Lučivjanský, M. Borovský, and M. Žukovič, Phase transitions in a frustrated Ising antiferromagnet on a square lattice, *Physical Review E* **91**, 032145 (2015).
- [13] N. Kellermann, M. Schmidt, and F. M. Zimmer, Quantum Ising model on the frustrated square lattice, *Physical Review E* **99**, 012134 (2019).
- [14] A. Kalz, A. Honecker, and M. Moliner, Analysis of the phase transition for the Ising model on the frustrated square lattice, *Physical Review B* **84**, 174407 (2011).
- [15] S. Jin, A. Sen, and A. W. Sandvik, Ashkin-Teller Criticality and Pseudo-First-Order Behavior in a Frustrated Ising Model on the Square Lattice, *Physical Review Letters* **108**, 045702 (2012).
- [16] M. K. Ramazanov, A. K. Murtazaev, and M. A. Magomedov, Thermodynamic, critical properties and phase transitions of the Ising model on a square lattice with competing interactions, *Solid State Communications* **233**, 35 (2016).
- [17] H. Li and L.-P. Yang, Tensor network simulation for the frustrated $J_1 - J_2$ Ising model on the square lattice, *Physical Review E* **104**, 024118 (2021).
- [18] A. I. Guerrero, D. A. Stariolo, and N. G. Almarza, Nematic phase in the $J_1 - J_2$ square-lattice Ising model in an external field, *Physical Review E* **91**, 052123 (2015).
- [19] E. Domínguez, C. E. Lopetegui, and R. Mulet, Quantum cluster variational method and phase diagram of the quantum ferromagnetic $J_1 - J_2$ model, *Physical Review B* **104**, 014205 (2021).
- [20] M. Sadrzadeh, R. Haghshenas, S. S. Jahromi, and A. Langari, Emergence of string valence-bond-solid state in the frustrated $J_1 - J_2$ transverse field Ising model on the square lattice, *Physical Review B* **94**, 214419 (2016).
- [21] A. Bobák, E. Jurčišinová, M. Jurčišin, and M. Žukovič, Frustrated spin-1/2 Ising antiferromagnet on a square lattice in a transverse field, *Physical Review E* **97**, 022124 (2018).
- [22] B. E. Vugmeister and V. A. Stephanovich, New random field theory for the concentrational phase transitions with appearance of long-range order. Application to the impurity dipole systems, *Solid State Communications* **63**, 323 (1987).
- [23] D. Mertz, F. Celestini, B. E. Vugmeister, H. Rabitz, and J. M. Debierre, Coexistence of ferrimagnetic long-range order and cluster superparamagnetism in $\text{Li}_{1-x}\text{Ni}_{1+x}\text{O}_2$, *Physical Review B* **64**, 094437 (2001).
- [24] V. Spirin, P. L. Krapivsky, and S. Redner, Freezing in Ising ferromagnets, *Physical Review E* **65**, 016119 (2001).
- [25] J. Olejarz, P. L. Krapivsky, and S. Redner, Fate of 2D Kinetic Ferromagnets and Critical Percolation Crossing Probabilities, *Physical Review Letters* **109**, 195702 (2012).
- [26] T. Blanchard and M. Picco, Frozen into stripes: Fate of the critical Ising model after a quench, *Physical Review E* **88**, 032131 (2013).
- [27] O. Mustonen, S. Vasala, K. P. Schmidt, E. Sadrollahi, H. C. Walker, I. Terasaki, F. J. Litterst, E. Baggio-Saitovitch, and M. Karppinen, Tuning the $S=1/2$ square-lattice antiferromagnet $\text{Sr}_2\text{Cu}(\text{Te}_{1-x}\text{W}_x)\text{O}_6$ from Néel order to quantum disorder to columnar order, *Physical Review B* **98**, 064411 (2018).
- [28] D. Afanasiev, J. R. Hortensius, B. A. Ivanov, A. Sasani, E. Bousquet, Y. M. Blanter, R. V. Mikhaylovskiy, A. V. Kimel, and A. D. Caviglia, Ultrafast control of magnetic interactions via light-driven phonons, *Nature Materials* **20**, 607 (2021).
- [29] X. Li, T. Qiu, J. Zhang, E. Baldini, J. Lu, A. M. Rappe, and K. A. Nelson, Terahertz field-induced ferroelectricity in quantum paraelectric SrTiO_3 , *Science* **364**, 1079 (2019).
- [30] T. F. Nova, A. S. Disa, M. Fechner, and A. Cavalleri, Metastable ferroelectricity in optically strained SrTiO_3 , *Science* **364**, 1075 (2019).

Methods

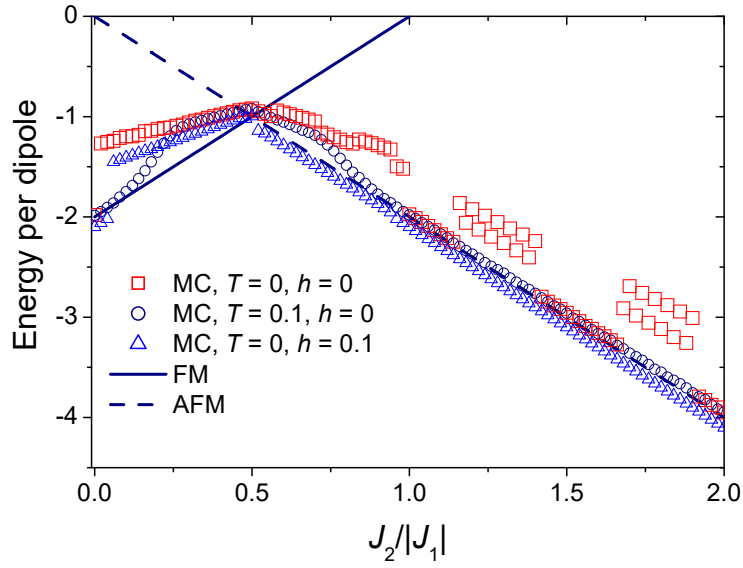
We perform Monte Carlo simulations with single-spin-flip Glauber dynamics at zero temperature and Metropolis dynamics at low temperatures, making a deep quench from a high-temperature (random) spin configuration, according to the following standard algorithm. If a randomly chosen spin flip leads to a negative energy change $\Delta E < 0$, then a new state is accepted. Otherwise, when $\Delta E \geq 0$, the probability of acceptance is

$\alpha = \exp(-\Delta E/T)$ for the Metropolis algorithm, and $\alpha/(1 + \alpha)$ for the Glauber dynamics. Both algorithms satisfy the detailed balance criteria and give the same final result. Periodic boundary conditions were used in all calculations and the sample size was equal to $L = 100$. To obtain the data in Fig. 2 and Extended Data Fig. 1, relaxation was performed at each temperature, starting from a random spin configuration, with 10^5 Monte Carlo steps per spin (MCS) used for thermalization and the same number of MCS for subsequent calculations of thermodynamic quantities for each run.

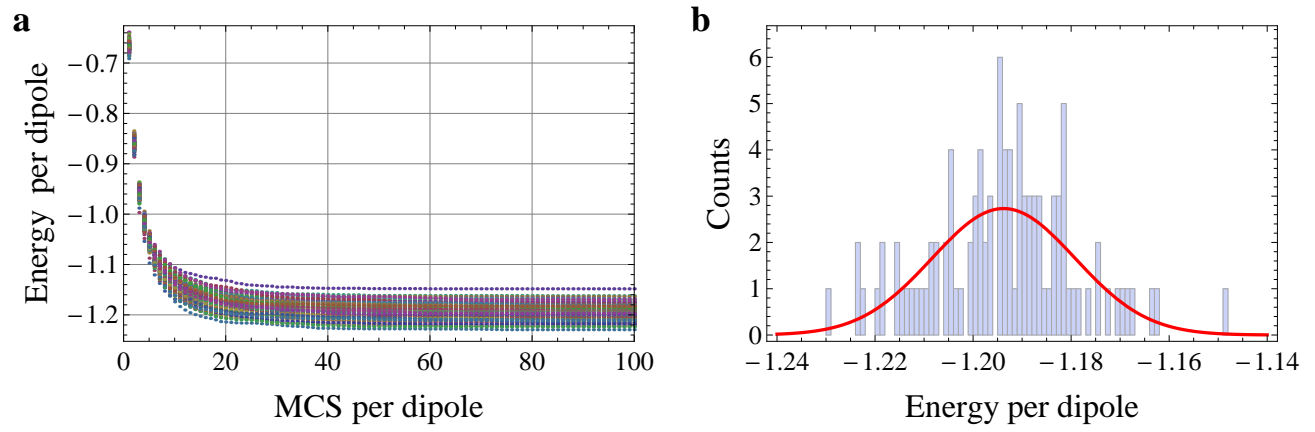
For staggered polarization, the largest of the values corresponding to the propagation vectors $\mathbf{q} = (0, \pi)$ and $\mathbf{q} = (\pi, 0)$ is taken. We also calculated the susceptibilities of N interacting spins via fluctuations of the average spin, $s = N^{-1} \sum_{i=1}^N s_i e^{i\mathbf{q}\mathbf{r}_i}$, with the propagation vector \mathbf{q} as $\chi = NT^{-1}(\langle s^2 \rangle - \langle s \rangle^2)$ and obtained critical temperatures from their maxima (Fig. 3a). When simulating at zero temperature (Fig. 3b), each data point was averaged over 100 samples with a relaxation time of 10^4 MCS (Extended Data Fig. 3).



Extended Data Fig. 1 | MC results for polarization and energy per dipole for different values of $p = J_2/|J_1|$. **a**, Uniform polarization (left y-axis) and energy per dipole (right y-axis) in a uniform field, $p < 1/2$. **b**, Staggered polarization and energy per dipole in a staggered field, $p > 1/2$. Open markers correspond to polarization, filled markers indicate energy. Purple triangles correspond to the field magnitude $h = 0.001$, blue dots correspond to the absence of a field. Each data point is derived from a single MC run with a random initial state at each temperature.



Extended Data Fig. 2 | Energy per dipole obtained by MC simulations for different values of the ratio $p = \mathbf{J}_2/|\mathbf{J}_1|$. Red squares correspond to zero temperature and no field, dark blue circles and blue triangles correspond to $T = 0.1$, $h = 0$, and $T = 0$, $h = 0.1$, respectively. The applied external field is uniform for $p < 1/2$, and it is staggered for $p > 1/2$. The standard deviations of the energy distribution histogram over 100 samples is smaller than the markers (Extended Data Fig. 3). Dark blue solid and dashed lines correspond to the energy of the FM and AFM states at $h = 0$. For $T = 0$, $h = 0.1$, the transition between stable and metastable states occurs around $p_{\text{FM}} = 0.05$ and $p_{\text{AFM}} = 0.95$.



Extended Data Fig. 3 | Monte Carlo simulation for $J_2/|J_1| = 0.1$ at zero temperature. **a**, Energy relaxation for 100 samples. **b**, Final energy histogram and superimposed Gaussian function with a calculated mean value of $\langle E \rangle = -1.19$ and a standard deviation of $\sigma_E = 0.015$.